

Cot/tpl2 (MAP3K8) Mediates Myeloperoxidase Activity and Hypernociception following Peripheral Inflammation^{*[S]}

Received for publication, July 29, 2010 Published, JBC Papers in Press, August 24, 2010, DOI 10.1074/jbc.M110.169409

Irene Soria-Castro^{†1}, Agnieszka Krzyzanowska[§], Marta López Pelaéz[‡], Javier Regadera[§], Gema Ferrer[‡], Lluís Montoliu[¶], Rosario Rodríguez-Ramos^{||}, Margarita Fernández[‡], and Susana Alemany^{‡2}

From the [†]Instituto de Investigaciones Biomédicas “Alberto Sols,” Consejo Superior de Investigaciones Científicas–Universidad Autónoma de Madrid (UAM), Madrid 28029, the [§]Departamento de Anatomía, Histología y Neurociencia Facultad Medicina, UAM, Madrid 28029, and the [¶]Departamento de Biología Molecular y Celular Centro Nacional de Biotecnología (CNB-CSIC) and the ^{||}Departamento Ciencias Médicas, Facultad Medicina, Universidad San Pablo, CEU, Boadilla del Monte, Madrid 28668, Spain

Cot/tpl2 (also known as MAP3K8) has emerged as a new and potentially interesting therapeutic anti-inflammatory target. Here, we report the first study of Cot/tpl2 involvement in acute peripheral inflammation *in vivo*. Six hours after an intraplantar injection of zymosan, Cot/tpl2^{-/-} mice showed a 47% reduction in myeloperoxidase activity, concomitant with a 46% lower neutrophil recruitment and a 40% decreased luminol-mediated bioluminescence imaging *in vivo*. Accordingly, Cot/tpl2 deficiency provoked a 25–30% reduction in luminol-mediated bioluminescence and neutrophil recruitment together with a 65% lower macrophage recruitment 4 h following zymosan-induced peritonitis. Significantly impaired levels of G-CSF and GM-CSF and of other cytokines such as TNF α , IL-1 β , and IL-6, as well as some chemokines such as MCP-1, MIP-1 β , and keratinocyte-derived chemokine, were detected during the acute zymosan-induced intraplantar inflammatory response in Cot/tpl2^{-/-} mice. Moreover, Cot/tpl2 deficiency dramatically decreased the production of the hypernociceptive ligand NGF at the inflammatory site during the course of inflammation. Most importantly, Cot/tpl2 deficiency significantly reduced zymosan-induced inflammatory hypernociception in mice, with a most pronounced effect of a 50% decrease compared with wild type (WT) at 24 h following intraplantar injection of zymosan. At this time, Cot/tpl2^{-/-} mice showed significantly reduced NGF, TNF α , and prostaglandin E₂ levels compared with WT littermates. In conclusion, our study demonstrates an important role of Cot/tpl2 in the NGF, G-CSF, and GM-CSF production and myeloperoxidase activity in the acute inflammatory response process and its implication in inflammatory hypernociception.

Activation of the pattern recognition receptors, which include Toll-like receptors (TLRs),³ RIG-I-like receptors, NOD-

like receptors, and C-type lectin receptors, by pathogen-associated molecular patterns starts a program that culminates in the development of an inflammatory process (for review, see Ref. 1). TLRs as well as IL-1 receptors, despite their marked differences in their extracellular regions, have a conserved cytoplasmic Toll/IL-1 receptor domain (for review, see Ref. 2). Cot/tpl2, also known as MAP3K8, is the sole MAP3K that activates the MKK1/2-ERK1/2 pathway in response to stimulation of the TLR/IL-1 receptor superfamily, as well as in response to the activation of some receptors of the TNF family (3–10). However, Cot/tpl2 does not participate in the activation of ERK1/2 by stimulation of the C-type lectin receptor dectin-1 (11).

In resting cells, Cot/tpl-2 forms a stable and inactive complex with p105 NF- κ B and ABIN2 (A20-binding inhibitor of NF- κ B2), among other proteins, to protect Cot/tpl-2 from degradation. Adequate TLR/IL-1 receptor stimulation induces the activation of the IKK complex; active IKK β kinase phosphorylates p105 NF- κ B, triggering its partial degradation to p50 NF- κ B (12–15). Cot/tpl2 is then dissociated from the complex and with an adequate phosphorylation state (16–19) is capable of activating MKK1 and consequently ERK1/2 (6, 20–22) prior to being rapidly degraded through the proteasome pathway (6, 20, 23). Cot/tpl2 is required to process pre-TNF α to its mature secreted form in LPS-stimulated macrophages (24). In addition, in different isolated cell types Cot/tpl2 controls the secretion of other cytokines and chemokines such as IL-8, MCP-1, MIP-1 β , KC, and IL-6 (3, 10, 24–27). Moreover, Cot/tpl2 activation is necessary for the production of PGE₂ in LPS-stimulated macrophages (9). By studying Cot/tpl2-deficient mice, Cot/tpl2 has been demonstrated to participate in LPS-induced septic shock (7) and inflammatory bowel disease *in vivo* (28). Hence, Cot/tpl2 fulfills a role in innate and adaptive immunity that cannot be replaced by any other protein.

The MAP kinase ERK1/2 participates in many different biological processes. The precise biological role in which ERK1/2 is involved is given by the nature of the extracellular signal and consequently the MAP3K, such as Raf or Cot/tpl2 that triggers its activation. Cot/tpl2 provides an alternative, independent of other MKK1/2 kinases, mode of MKK1-ERK1/2 activation, thus providing a more specific target for pharmacological manipulation, without fully disturbing the ERK1/2 function. Thus, Cot/tpl2 has emerged as an attractive target to develop new and improved anti-inflammatory drugs (29, 30). Indeed, there is now enormous interest in the develop-

* This work was supported by Comunidad de Madrid Grants SAF 2008-00819 and Mutua Madrileña.

[S] The on-line version of this article (available at <http://www.jbc.org>) contains supplemental Figs. 1–5.

¹ Recipient of the Formación Personal Investigador fellowship.

² To whom correspondence should be addressed: Susana Alemany, IIBM CSIC-UAM, Arturo Duperier 4, 28029 Madrid, Spain. Fax: 34 91 585 4401; E-mail: salemany@iib.uam.es.

³ The abbreviations used are: TLR, Toll-like receptor; BMDM, bone marrow-derived macrophages; LTB₄, leukotriene B₄; MPO, myeloperoxidase; PGE₂, prostaglandin E₂; MCP-1, monocyte chemoattractant protein-1; MIP-1 β , macrophage inflammatory protein-1 β ; KC, keratinocyte-derived chemokine.

Cot/tpl2 Regulates Inflammatory Hypernociception

ment of small compounds specifically to block Cot/tpl2 activity to identify new therapeutic anti-inflammatory agents (31–36).

Zymosan has been extensively used as an inducer of acute inflammation in mouse hindpaws. Here, we show that Cot/tpl2 mediates zymosan-induced inflammatory processes *in vivo*, and, as inflammation often results in the development of pain, Cot/tpl2 is involved in the maintenance of inflammatory hypernociception in mice. Furthermore, we also demonstrate that Cot/tpl2 modulates the number of neutrophils recruited to inflammatory foci induced by zymosan injection *in vivo* as well as the level of cytokines/chemokines, NGF, PGE₂, and leukotriene (LT) B₄ production at those sites.

EXPERIMENTAL PROCEDURES

Animals and Models of Inflammation—C57BL/6J WT and C57BL/6J Cot/tpl2^{-/-} littermates were produced from heterozygotic mice, and their genotype was determined by PCR. Male WT and Cot/tpl2^{-/-} mice 10–14 weeks old were used in the experiments. The zymosan-induced paw inflammation model was employed by injecting freshly prepared zymosan (300 μg, 30 μl of PBS; Invivogen) into the plantar region of the left hindpaw to induce inflammation; peritoneal inflammation was induced by injecting freshly prepared zymosan (1 mg, 500 μl of PBS) intraperitoneally. Intraplantar tissue samples were rinsed with saline and fixed by immersion in 4% formalin for 24 h before they were dehydrated in alcohol, clarified in xylene, and embedded in paraffin. Histological paraffin sections (5 μm) were stained with Masson's trichrome for analysis. Sections were studied with an Olympus Optical BX-50 microscope, using planapochromatic 100× lens for bright-field observation. Photomicrographs of selected fields were performed with an Olympus DP 70, 12-bit digital camera.

Hindpaw Intraplantar Extracts and Intraplantar Cell Isolation—Approximately 0.5 cm² of plantar tissue was harvested and frozen immediately in liquid nitrogen. The plantar tissue was homogenized in 1 ml of buffer (0.05% Tween 20, 10 mM EDTA (pH 7.5) in PBS) to measure NGF as well as different cytokines and chemokines. For RNA extraction, tissues were resuspended in 1 ml Trizol and for Western blot analysis in the lysis buffer described previously (37). The different samples were triturated in special tubes with matrix Lysing A (MP, Biomedicals) through three cycles of 6 s on ice in the Fastprep-24 apparatus (MP, Biomedicals). The different homogenized extracts were subjected to a centrifugation at 14,000 × g for 10 min at 4 °C, and supernatants were frozen at -80 °C until used. COX2 mRNA levels were determined by quantitative RT-PCR analysis using specific COX2 TaqMan primers (Applied Biosystems). Cot/tpl2 protein expression was determined in homogenized intraplantar extracts as described previously (37). Intraplantar cells were isolated as described previously with some minor modifications (38, 39). Briefly, intraplantar tissue corresponding to six hindpaws was digested for 1 h at 37 °C in 800 μl of RPMI 1640 medium containing 10% FBS, 3 mg/ml collagenase (Sigma), and 1 mg/ml hyaluronidase (Sigma), with constant gentle rocking. The digested fragments were pressed through a 50-μm nylon filter (BD Biosciences) to remove particles. Isolated cells were washed twice in PBS and subjected to flow cytometry analysis using the antibodies described below

and according to a previously published method (40) with Tru-Count tubes (BD Biosciences). Control experiments showed that incubation of peritoneal cells with collagenase and hyaluronidase for 1 h at 37 °C did not alter the surface antigen phenotype of the cells (data not shown).

Luminol-mediated Bioluminescence Imaging in Vivo and Measurement of Myeloperoxidase Activity in Intraplantar Extracts—The bioluminescence generated after luminol intraperitoneal injection was measured in the whole animals as described previously (41). Briefly, after the intraplantar or intraperitoneal zymosan injection, luminol (5 mg/100 μl; Sigma) was intraperitoneally injected, and the bioluminescence was recorded in an IVIS lumina at the times indicated (Xenogen). To avoid the absorption of the bioluminescence by the black skin of the C57BL/6J mice, zymosan-induced peritonitis was performed in the C57 albinos [B6(Cg)-Tyr<c-2>/J C57] WT and Cot/tpl2^{-/-} mice. Myeloperoxidase (MPO) activity was measured as described previously (42) with some minor modifications. Briefly, intraplantar tissue was pulverized in liquid N₂ and then homogenized in PBS and subsequently snap-frozen in dry ice and thawed on three consecutive occasions. Debris were removed by a centrifugation at 2,000 × g for 20 min at 4 °C, and the supernatant was frozen at -20 °C. Measurement of MPO activity was performed in triplicate using 50 μl of intraplantar extracts or 50 μl of PBS with 0.5% HTAB, 150 μl of PBS, 15 μl of 0.22 M Na₂PO₄, 20 μl 0.034% H₂O₂, and 20 μl of 18 mM TMB (Sigma) diluted in 8% dimethylformamide. After a 5-min incubation at 37 °C the reaction was terminated with H₂SO₄ (50 μl, 0.18M), and absorbance measured (450 nm). Protein concentration was determined as described previously (37).

Western Blotting of Bone Marrow-derived Macrophage Extracts—Bone marrow derived macrophages (BMDM) were cultured as described previously (43), stimulated with zymosan (10 μg/ml), and at the times indicated, the cell supernatants were frozen in liquid nitrogen, and the cells (5 × 10⁶) were utilized to prepare extracts for analysis in Western blots (37) using anti-COX2 (Santa Cruz Biotechnology) and anti-ERK2 (Santa Cruz Biotechnology) antibodies.

Flow Cytometry Analysis of Cytokines/Chemokines and of Isolated Cells—Lavage of the peritoneal cavity was performed with 3 ml of PBS, and after a 30-s gentle manual massage, the peritoneal exudate containing fluid and leukocytes was retrieved. After centrifugation, the peritoneal fluid was used to evaluate the concentration of different chemokines and cytokines by FACS analysis. Cells obtained from the peritoneal lavages were washed twice in PBS, counted by two independent investigators blind to the source of the samples, and resuspended in 1 ml of PBS with 0.5% BSA. For phenotype analysis, peritoneal or intraplantar isolated cells (0.3–0.5 × 10⁶ cells/test) were pre-treated with CD16/32 (2.4G2, Fc block; Culti) for 20 min in ice, and they were subsequently stained with antibodies raised against the following proteins at a concentration of 5 μg/ml: F4/80 (rat anti-mouse; eBioscience) for macrophage detection, Ly-6G (rat anti-mouse; Pharmingen) for neutrophil identification or their corresponding isotype controls (Pharmingen). The samples were analyzed by flow cytometry after multiple washing, and the data were examined using the CXP program. To

quantify simultaneously the concentration of TNF α , IL-1 β , IL-6, MIP-1 α , MIP-1 β , KC, MCP-1, G-CSF, and GM-CSF in plantar tissue extracts, culture supernatants or in peritoneal exudates, CBA Cytometric (BD Biosciences) kits were utilized. Fluorescence intensities were assayed by flow cytometry in a FACS Canto Cytometer (BD Biosciences), and they were compared with a standard curve generated for each cytokine to determine the concentration in each sample. The data were analyzed utilizing the FCAP Array program (BD Biosciences).

NGF, PGE₂, and LTB₄ Measurement—NGF levels were determined in mouse hindpaw extracts using the mouse NGF Sandwich ELISA kit (Millipore), according to the manufacturer's instructions. PGE₂ and LTB₄ were measured in BMDM culture supernatants and in tissue plantar extracts using commercially available PGE₂ and LTB₄ enzyme immunoassay kits (Cayman Chemicals). The analysis was performed by the company blind to the source of the samples.

Measurement of Hindpaw Swelling and Evans Blue Extravasation—The maximal dorso-plantar thickness and medial-lateral width measured proximal to the toes were determined at different times after zymosan (left hindpaw) or saline (right hindpaw) injection using a digital caliper (Starrett). This instrument has a resolution of 0.05 mm. Evans Blue plasma extravasation was studied as described previously (44). Briefly, Evans Blue (50 mg/kg) was injected intravenously into the lateral tail vein and immediately afterward, zymosan was intraplantar-injected into the left hindpaw and PBS into the right hindpaw. After 4 h, the intraplantar tissue was removed, chopped up, and incubated in formamide for 24 h at 56 °C. The Evans Blue extracted was measured spectrophotometrically at 600 nm.

Behavioral Procedures—Behavioral tests were performed in a low lit and quiet room, always by the same researcher who was blind to the treatment. On the day of the behavioral experiments, the animals were habituated to the apparatus for at least 30 min before beginning the behavioral testing. The animals were placed in Plexiglas chambers (12 × 8 × 16 cm) with a wire mesh floor, and the plantar surface of the hindpaw was stimulated using a hand-held force transducer (electronic anesthesiometer, IITC Life Science) with a semiflexible polypropylene probe tip (0.5-mm² diameter). The probe was applied perpendicular to the central area of the paw, gradually increasing the force until the animal withdrew its foot with a clear flinching action. The left and right hindpaws were stimulated alternatively three times, at intervals of at least 1 min, and the average score of the three readings was taken as the threshold value for paw withdrawal. All mice were tested before any inflammatory procedure to establish a baseline level of responsiveness. In the zymosan experiment, the baseline withdrawal threshold was 6.9 ± 0.2g ($n = 16$). The results are presented as the difference in withdrawal thresholds (in grams) before ($t = 0$) and after injection of the inflammatory agents. The behavioral analysis was performed 3, 6, 24, and 48 h after zymosan injection.

Statistical Analysis—The results are presented as the means ± S.E. The behavioral outcomes were compared by means of a two-way ANOVA with a Tukey post hoc test, and the rest of the data were analyzed with Student's t test. Values were taken to be statistically significant at $p < 0.05$ (*, $p < 0.05$; **, $p < 0.01$; ***, $p < 0.001$).

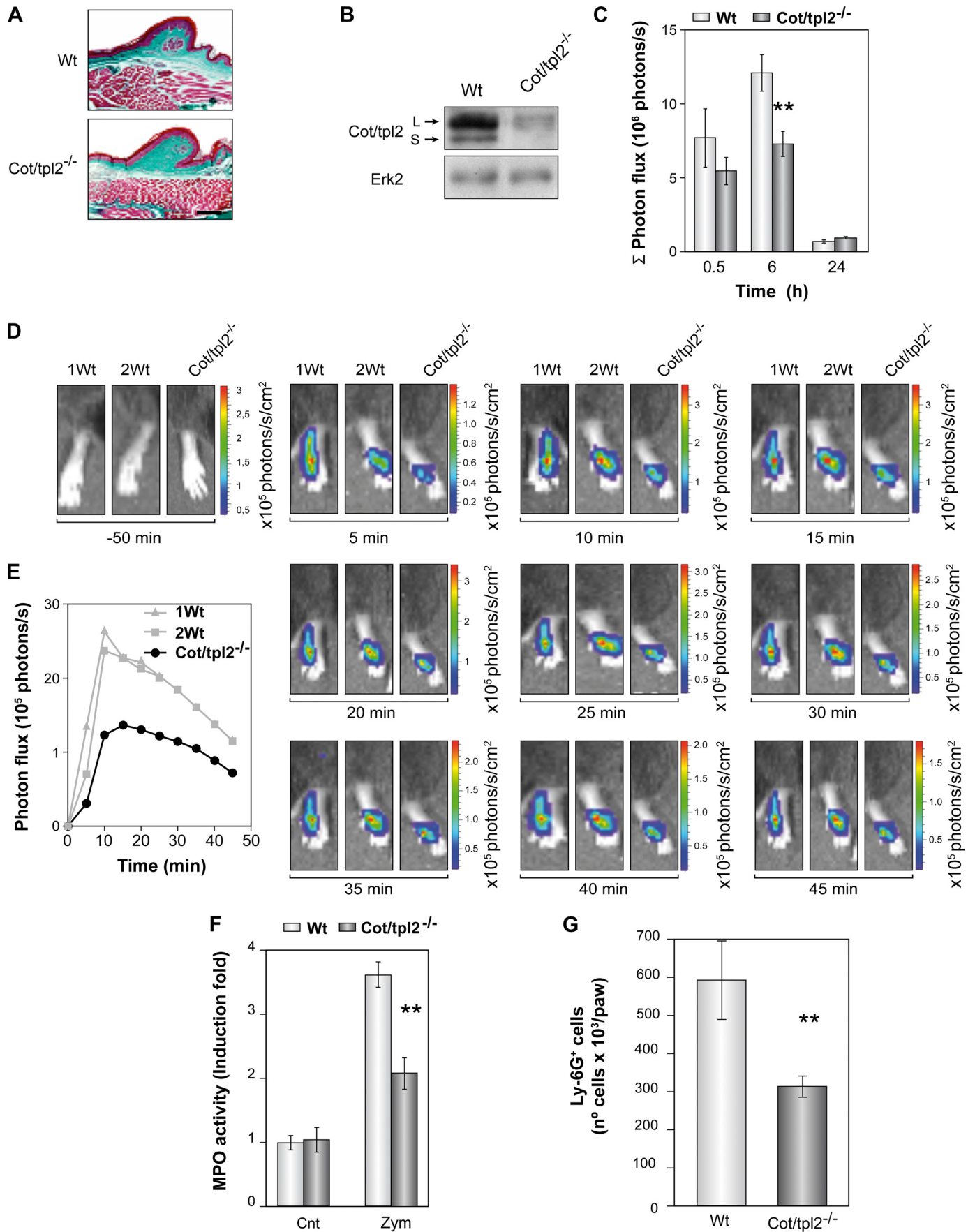
RESULTS

Cot/tpl2 Modulates Zymosan-induced MPO Activity in Mice Hindpaws—Zymosan stimulates both dectin-1 and TLR2/6 receptors. Thus, to ensure a role of Cot/tpl2 in the zymosan intracellular signaling through TLR2/6, we stimulated WT and Cot/tpl2^{-/-} BMDM, which express low levels of dectin-1 but high levels of TLR2/6 (45), with zymosan and found no increase in the phosphorylation state of ERK1/2 in Cot/tpl2^{-/-} BMDM (supplemental Fig. S1). Moreover, we ensured that Cot deficiency does not modify the normal stratified skin epithelium or epidermal-dermal organization in the hindpaws of the mice (Fig. 1, A and B).

MPO is one of the principal components of the azurophilic granules in neutrophils, and as such, it has been extensively used as a marker of neutrophil infiltration and acute inflammation (46, 47). Luminol-mediated bioluminescence *in vivo* has been recently reported to determine the MPO activity at the inflamed site (41), thus the amount of bioluminescence produced after the luminol intraperitoneal injection was determined *in vivo* 0.5, 6, and 24 h following the injection with zymosan in the plantar region of the WT and Cot/tpl2^{-/-} mice left hindpaw. There was a significant decrease in the bioluminescence generated in Cot/tpl2^{-/-} hindpaws 6 h after the injection of zymosan (Fig. 1, C–E). The bioluminescence observed 24 h later in both WT and Cot/tpl2^{-/-} hindpaws had returned to almost basal levels (Fig. 1C). In concordance with these data, Cot/tpl2^{-/-} hindpaw extracts 6 h following zymosan injection showed a 47% decreased MPO specific activity compared with zymosan-injected WT hindpaws extracts (Fig. 1F). Because this decrease in MPO activity in Cot/tpl2^{-/-} hindpaws could indicate a decrease in the number of infiltrated neutrophils, the number of inflammatory cells was determined in zymosan-injected WT and Cot/tpl2^{-/-} hindpaws. To this end, WT and Cot/tpl2^{-/-} intraplantar tissues 6 h following intraplantar injection of zymosan were subjected to collagenase and hyaluronidase digestion, and isolated cells were subsequently subjected to flow cytometry analysis (supplemental Fig. S2). Cot/tpl2^{-/-} inflamed intraplantar tissue showed 46% less neutrophils (Ly-6G⁺F4/80⁻) than their WT counterpart (Fig. 1G), whereas no neutrophils could be detected in control WT and Cot/tpl2^{-/-} hindpaws (data not shown).

Altered Inflammatory Cell Recruitment after Intraperitoneal Zymosan Injection in Cot/tpl2^{-/-} Mice—To establish further the role of Cot/tpl2 in the recruitment of inflammatory cells, the number of cells recruited in response to zymosan-induced peritonitis was evaluated in WT and Cot/tpl2^{-/-} mice. A similar number of cells were observed in the peritoneum of WT and Cot/tpl2^{-/-} mice 2 h after the initiation of inflammation (Fig. 2A), and even though after 4 h the number of cells recruited to the peritoneal cavity increased, Cot/tpl2^{-/-} mice showed 25% less cell recruitment. Flow cytometry analysis of these cells demonstrated a significant decrease in the proportion of macrophages (F4/80⁺Ly-6G⁻) in Cot/tpl2^{-/-} mice, whereas the percentage of neutrophils (Ly-6G⁺F4/80⁻) was similar in both groups (Fig. 2, B and C). Nevertheless, when the reduction in the total number of cells recruited from the peritoneum of Cot/tpl2^{-/-} mice was taken into account, Cot/

Cot/tpl2 Regulates Inflammatory Hypernociception



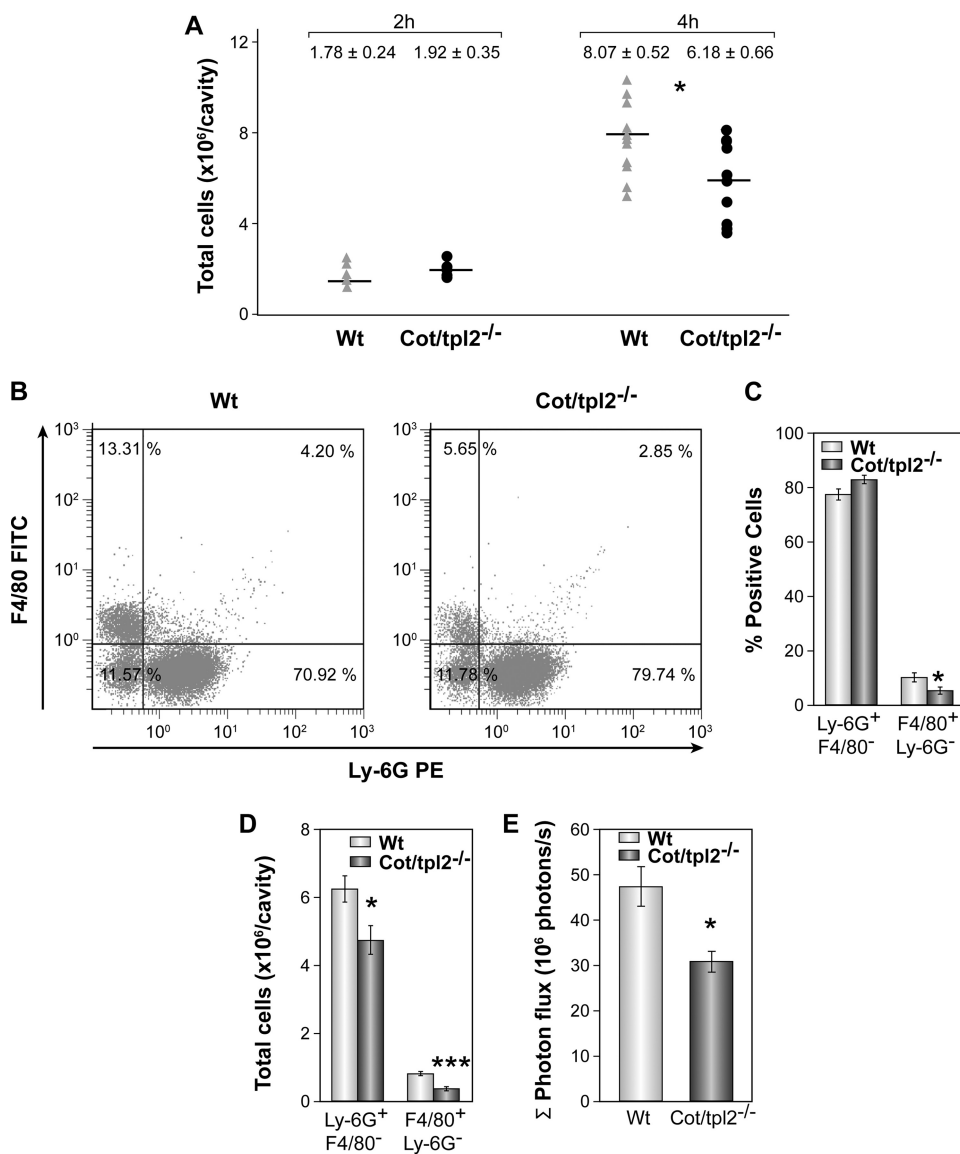


FIGURE 2. Recruitment of inflammatory cells during zymosan-induced peritonitis in WT and Cot/tpl2^{-/-} mice. Animals were injected intraperitoneally with zymosan (1 mg, 500 μ l of PBS), killed 2 or 4 h later, and the peritoneal cells were obtained. **A**, total number of cells recruited at 2 and 4 h after zymosan-induced peritonitis in WT and Cot/tpl2^{-/-} mice (2 h, $n = 5$ each group; 4 h, $n = 9$ each group). **B**, representative FACS profile of F4/80⁺Ly-6G⁻ versus Ly-6G⁺F4/80⁻ staining of total isolated intraplantar cells obtained 6 h after the zymosan injection (left panel, WT; right panel, Cot/tpl2^{-/-} mice). Data are representative of six independent WT and Cot/tpl2^{-/-} animals. **C**, means \pm S.E. (error bars) of the Ly-6G⁺F4/80⁺ (neutrophils) and F4/80⁺Ly-6G⁻ (macrophages) cells recruited at 4 h from the peritoneum of WT and Cot/tpl2^{-/-} mice ($n = 6$ for each group). **D**, total number of Ly-6G⁺F4/80⁻ and F4/80⁺Ly-6G⁻ cells calculated using the formula: % positive cells \times 0.01 \times total cell number obtained in **A**. The graph shows the means \pm S.E. of six animals/group.

tpl2 deficiency not only provoked a decrease of approximately 65% in the number of macrophages recruited but also, a decrease of approximately 25% in the total number of neutrophils recruited (Fig. 2D). Accordingly, Cot/tpl2^{-/-} mice

showed approximately 30% less luminol-mediated bioluminescence *in vivo* 4 h after the intraperitoneal injection of zymosan (Fig. 2E and supplemental Fig. S3). Recent evidences point to MPO to control the inflammation by activating the neutrophils through its association with integrin CD11b/CD18, with MPO emerging as a mayor player controlling inflammation (48–51). Nevertheless, it should be noted that no significant differences were observed in the expression of CD11b in WT and Cot/tpl2^{-/-} macrophages or neutrophils (supplemental Fig. S4).

Modulation of Chemokine and Cytokine Production by Cot/tpl2 Deficiency *In Vivo*—The release of the chemokines MIP-1 β , MIP-1 α , MCP-1, and KC at the acute inflammatory focus is responsible for the recruitment of inflammatory cells (52, 53). Thus, we analyzed the role of Cot/tpl2 in the secretion of these chemokines induced by zymosan in the intraplantar tissue. MIP-1 β concentration decreased significantly within the first 2 h of zymosan injection in the intraplantar tissue of Cot/tpl2^{-/-} mice (Fig. 3). By contrast, both WT and Cot/tpl2^{-/-} hindpaws had similar levels of MIP-1 α during the progression of inflammation (Fig. 3). A significant decrease in MCP-1 levels was observed 5 h after zymosan injection in the hindpaws of Cot/tpl2^{-/-} mice compared with zymosan-injected WT hindpaws, whereas in zymosan-injected Cot/tpl2^{-/-} intraplantar tissue KC levels were reduced by 25% with respect to the WT intraplantar tissue 2 h after the initiation of inflammation (Fig. 3).

Taking into account the established role of GM-CSF and G-CSF in recruiting and also maintaining macrophages and neutrophils active at the inflammatory site (54–56), we also

FIGURE 1. MPO activity in the hindpaws of zymosan-injected WT and Cot/tpl2^{-/-} mice. **A**, sections of naive hindpaws from WT and Cot/tpl2^{-/-} mice stained with Masson's trichrome. Scale bar, 100 μ m. **B**, Western blots of naive intraplantar lysates from WT and Cot/tpl2^{-/-} mice. **C**, means \pm S.E. (error bars) of the Σ of the photon flux generated by the intraperitoneal injection of luminol at different times after zymosan injection (0.5, 6, and 24 h) in the hindpaws of WT and Cot/tpl2^{-/-} mice ($n = 8$ for each type of mice). **D**, luminol-mediated bioluminescence images of the hindpaws from WT and Cot/tpl2^{-/-} mice 6 h after the intraplantar zymosan injection. The images have been taken before and between 5 and 45 min after intraperitoneal injection of luminol at 5-min intervals (one representative experiment with one Cot/tpl2^{-/-} and two from WT mice is shown). **E**, representation of the photon flux recorded in **D**. **F**, measurement of MPO activity in the intraplantar tissue extracts of WT and Cot/tpl2^{-/-} mice hindpaws 6 h following zymosan (Zym) or just PBS (Cnt) injection. The value 1 is given to O.D./mg protein of WT intraplantar extracts injected only with PBS. The means \pm S.E. of three independent experiments of four different pooled tissue extracts from each condition are shown. **G**, total number of Ly-6G⁺F4/80⁺ isolated from WT and Cot/tpl2^{-/-} intraplantar tissue 6 h following zymosan injection. The means \pm S.E. of four independent experiments of six different pooled digested intraplantar tissues are shown.

Cot/tpl2 Regulates Inflammatory Hypernociception

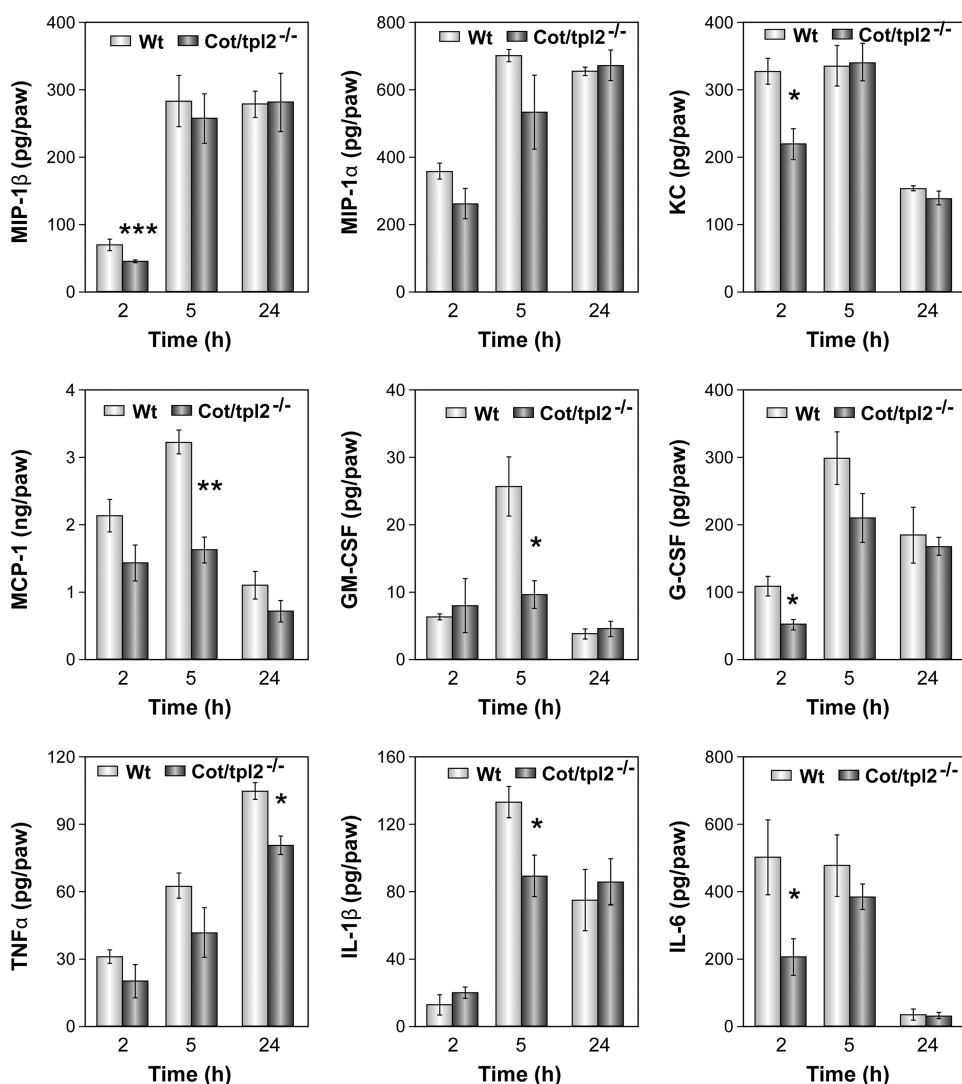


FIGURE 3. Zymosan induction of cytokines and chemokines in intraplantar tissues of WT and Cot/tpl2^{-/-} mice. The concentration of MIP-1β, MIP-1α, KC, MCP-1, GM-CSF, G-CSF, TNFα, IL-1β, and IL-6 in the intraplantar tissue extracts of WT and Cot/tpl2^{-/-} mice was determined 2, 5, and 24 h after the injection of zymosan by FACS analysis with the CBA system. The means ± S.E. (error bars) of three independent experiments of three different pooled tissues extracts from each condition are shown.

studied the possible role of Cot/tpl2 in modulating the levels of these mediators at the inflammatory site. In the hindpaws of WT mice, maximal levels of GM-CSF were detected 5 h after zymosan injection, and at this time, the GM-CSF levels in Cot/tpl2^{-/-} were decreased significantly. Similarly, a decrease in G-CSF in the hindpaws of Cot/tpl2-deficient mice was detected 2 h after zymosan injection.

TNFα, IL-1β, and IL-6 are the main proinflammatory cytokines that activate the nociceptive terminals that innervate the inflamed tissues (52, 53, 57). Thus, we also decided to evaluate their levels during the course of zymosan-induced hindpaw inflammation. In zymosan-injected hindpaws of Cot/tpl2^{-/-} mice there was a tendency to produce lower TNFα, with a significant reduction of approximately 20% 24 h following zymosan injection compared with WT littermates (Fig. 3). A significant 30% decrease in IL-1β in zymosan-injected hindpaws of Cot/tpl2^{-/-} mice was evident at 5 h. Furthermore, Cot/tpl2 deficiency also provoked lower levels of IL-6 within the first 2 h after intraplantar zymosan-induced inflammation (Fig. 3).

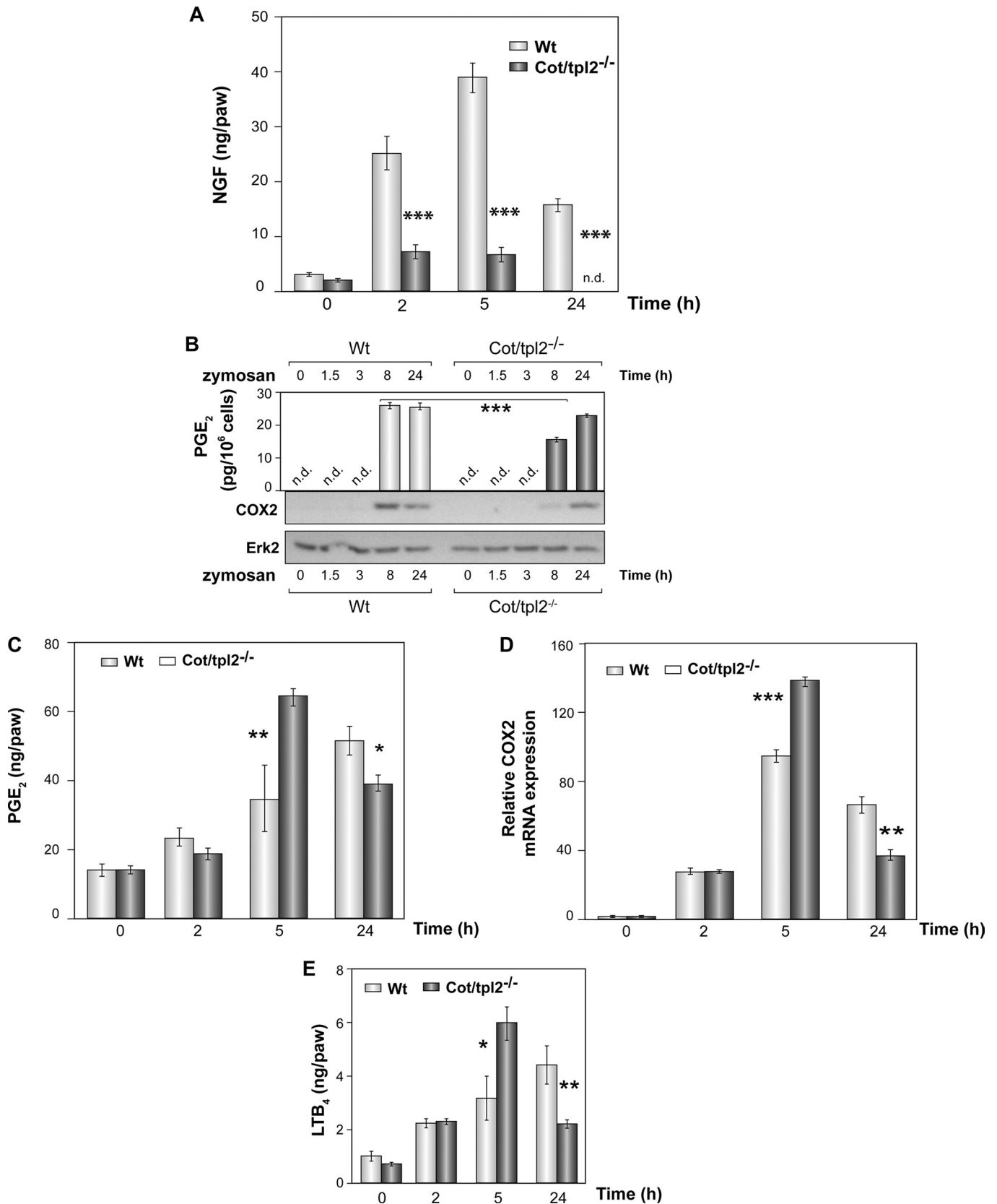
NGF, PGE₂, and LTB₄ Production in Zymosan-injected Intraplantar Tissue of WT and Cot/tpl2^{-/-} Mice—NGF and PGE₂ are key participants in the pain sensitization at the inflamed site (52, 53, 58). The rapid increase of NGF at the inflammatory site is dependent on, among other signals, the concentration of IL-1β and TNFα (58–60). The quantification of NGF levels during the progression of inflammation in zymosan-injected WT and Cot/tpl2^{-/-} hindpaws showed that Cot/tpl2 is a master regulator of the production of this pronociceptive factor (Fig. 4A).

On the basis of Cot/tpl2 capacity to trigger PGE₂ as well as TNFα production in LPS-stimulated BMDM, Cot/tpl2 has been proposed as a new interesting anti-inflammatory target (29, 30). Indeed, COX2 expression is impaired in Cot/tpl2-deficient BMDM within the first 10 h of LPS stimulation (9). Likewise, COX2 protein and PGE₂ production were also impaired in zymosan-stimulated Cot/tpl2^{-/-} macrophages 8 h after zymosan stimulation. However, after 24 h only a minor decrease in PGE₂ levels was evident in Cot/tpl2^{-/-} BMDM, and there were no significant differences in the levels of COX2 in Cot/tpl2^{-/-} compared with WT littermates (Fig. 4B). More importantly, the levels of PGE₂ in the extracts of zymosan-injected intraplantar tissues from both WT and Cot/tpl2^{-/-} mice unexpectedly showed that Cot deficiency increased the concentration of PGE₂ 2-fold 5 h after the intraplantar injection of zymosan; however, 24 h following zymosan injection a 25% decrease was observed (Fig. 4C). These data correlated with the levels of COX2 mRNA detected in the zymosan-injected intraplantar tissue of Cot/tpl2^{-/-} mice (Fig. 4D). LTB₄ is involved in the expression of PGE₂ in zymosan-induced joint hypernociception (61), and thus, LTB₄ was measured at different times after zymosan injection in WT and Cot/tpl2^{-/-} hindpaws. Cot/tpl2 deficiency was associated with an increase in LTB₄ levels at 5 h, although there was a significant decrease 24 h later (Fig. 4E). LTB₄ could not be detected in either zymosan-activated WT or Cot/tpl2^{-/-} BMDM at any of the different times (0, 1.5, 3, 8, and 24 h) tested (data not shown).

Induction of Edema Formation in Zymosan-injected Hindpaws of WT and Cot/tpl2^{-/-} Mice—The formation of edema is a sign of inflammation, and there was a significantly smaller increase in both medio-lateral width and dorso-

plantar thickness in the zymosan-injected hindpaws of *Cot/tpl2*^{-/-} mice than in WT 3 h after intraplantar zymosan injection (Fig. 5, *A* and *B*). Accordingly, plasma extravasation

as measured by Evans Blue outflow revealed significantly less extravasation in the paws of *Cot/tpl2*^{-/-} mice 4 h after the intraplantar injection of zymosan (Fig. 5*C*). Nevertheless,



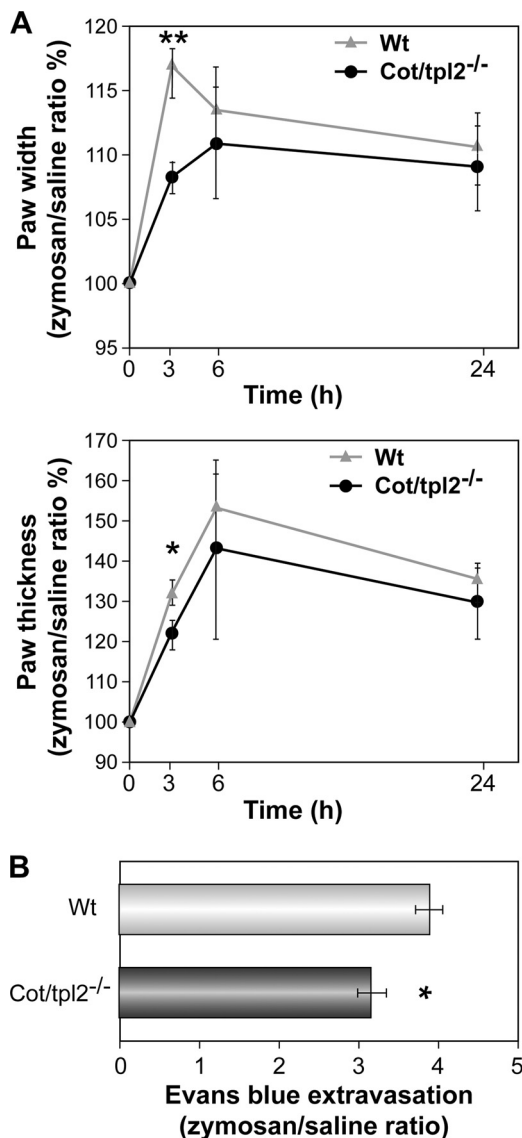


FIGURE 5. Paw edema following the induction of inflammation by zymosan in hindpaws of WT and Cot/tpl2^{-/-} mice. *A*, width and thickness of zymosan (*left*) and PBS (*right*) injected hindpaws from WT and Cot/tpl2^{-/-} mice before and at different times after injection. The values of hindpaw width and thickness are expressed as the value between the diameter measured after induction of inflammation divided by the basal (before) diameter in millimeters. Data are shown as the means \pm S.E. ($n = 7$), the value obtained before the injection being considered as 100%. *B*, quantification of Evans Blue extravasation over 4 h in zymosan-injected hindpaws from WT and Cot/tpl2^{-/-} mice. Values of Evans Blue extravasation are expressed as the values between the inflamed plantar tissue and its corresponding control. The graph represents means \pm S.E. (*error bars*) ($n = 9$ for each condition).

similar levels of swelling were observed between the hindpaws of WT and Cot/tpl2^{-/-} mice 6 h and 24 h after the induction of inflammation.

Cot/tpl2 Is Involved in Inflammatory Hypernociception in Mice—Finally, we evaluated how the aforementioned modulation of cytokine/chemokine, NGF, and PGE₂ production at the inflammatory site observed *in vivo* as a consequence of the deficiency of Cot/tpl2, affects the whole process of acute inflammation. Inflammatory pain is characterized by hypernociception whereby the intensity of the sensitization to a painful stimulus is preceded by and is directly dependent on the recruitment of inflammatory cells and the release of inflammatory cytokines and pronociceptive ligands (52, 53, 57). Thus, to evaluate the importance of Cot/tpl2 in inflammation *in vivo*, we quantified inflammatory hypernociception in the hindpaws of WT and Cot/tpl2^{-/-} mice intraplantar-injected with zymosan. Overall, there was a time-dependent reduction in mechanical hypernociception in Cot/tpl2^{-/-} mice compared with WT over a 48-h time course, with the most striking differences evident at 24 h after injection (Fig. 6). Furthermore, to evaluate the role of Cot/tpl2 in peripheral acute inflammation with a ligand that activates a TLR (TLR4), but not other pattern recognition receptors such as dectin-1, we also studied the role of Cot/tpl2 inflammatory hypernociception by injecting LPS into the hindpaws of the WT and Cot/tpl2^{-/-} mice, detecting again a significant decrease in LPS-induced hypernociception in Cot/tpl2-deficient mice (supplemental Fig. S5, *A* and *B*).

DISCUSSION

Cot/tpl2 controls ERK1/2 activation by TLR ligands, IL-1, and TNF α (3–8, 10, 62), and its inhibition does not affect the activation of the ERK1/2 pathway by other MAP3Ks. On the basis of its capacity to trigger PGE₂ and TNF α production, Cot/tpl2 has emerged as an attractive target to develop new and improved anti-inflammatory drugs (for review, see Refs. 29, 30). In this article we have studied the role of Cot/tpl2 in peripheral inflammation *in vivo*, demonstrating a role of Cot/tpl2 in inflammatory hypernociception and providing evidence of deficient neutrophil recruitment. MPO, one of the principal components of the azurophilic granules in neutrophils, has also emerged as a major factor controlling the acute inflammatory process (48–51), and our data demonstrate that Cot/tpl2-deficient mice show decreased luminol-mediated bioluminescence determined *in vivo* in two different zymosan-induced inflammation models and decreased MPO activity measured *in vitro* in intraplantar extracts of Cot/tpl2^{-/-} mice hindpaws injected with zymosan. This loss of MPO activity is in accordance with the lower number of recruited neutrophils at the inflamed site in Cot/tpl2^{-/-} mice. The impaired recruitment of cells induced by Cot/tpl2 deficiency is consistent with the decreased levels of different chemotactic factors (53–56, 63, 64) such as MIP-1 β ,

FIGURE 4. Involvement of Cot/tpl2 in the production of NGF, PGE₂, and LTB₄ synthesis by zymosan. *A*, concentration of NGF in the intraplantar tissue extracts of WT and Cot/tpl2^{-/-} mice hindpaws determined by ELISA 0, 2, 5, and 24 h after the injection of zymosan. The means \pm S.E. (*error bars*) of three independent experiments of three different pooled tissues extracts from each condition are shown. *B*, Western blot showing COX2 expression in WT and Cot/tpl2^{-/-} BMDM stimulated with zymosan (10 μ g/ml). As control of total protein, loaded total ERK2 levels were tested. One representative experiment of the four performed is shown. The PGE₂ concentration was measured in the supernatant of BMDM cells stimulated for 8 and 24 h. The means \pm S.E. of two independent determinations of three different pooled supernatants from each condition are shown. *C*, PGE₂ concentration in intraplantar tissues of WT and Cot/tpl2^{-/-} mice 0, 2, 5, and 24 h after injection with zymosan (300 μ g, 30 μ l). *D*, expression of COX2 mRNA detected by quantitative RT-PCR. Total RNA was extracted from zymosan-injected intraplantar tissues. The means \pm S.E. of two independent determinations of four different pooled tissue extracts from each condition are shown. *E*, LTB₄ concentration in the samples determined in *C*. *C* and *E*, means \pm S.E. of two independent measurements of four different pooled tissue extracts from each condition.

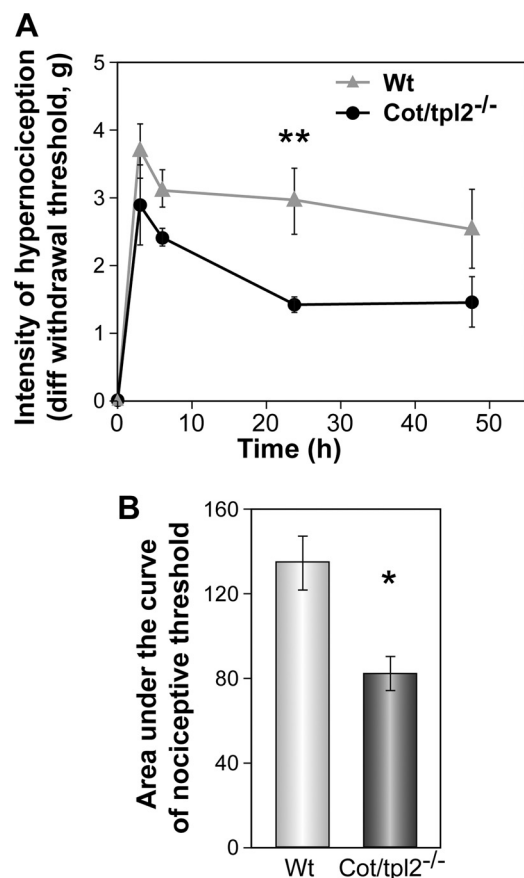


FIGURE 6. Cot/tpl2^{-/-} mice develop less hyperalgesia than the WT. Mechanical hypernociception was assessed following zymosan injection (300 μ g, 30 μ l) over a period of 48 h in WT ($n = 8$) and Cot/tpl2^{-/-} mice ($n = 7$). **A**, time-response curve of zymosan-induced hypernociception in WT and Cot/tpl2^{-/-} mice. The results are presented as the means \pm S.E. (error bars). **, $p = 0.004$, two-way ANOVA, Tukey post hoc. **B**, area under the curve graph. The changes in nociceptive threshold and withdrawal latency were calculated for each mouse as the area under the curve versus time (over a 48-h period), and the results are presented as the means \pm S.E. *, $p = 0.019$, Student's t test.

KC, G-CSF, and/or GM-CSF detected within the first 5 h of inflammation in Cot/tpl2^{-/-} mice.

Cot/tpl2 has an established essential role in the secretion of MCP-1, MIP-1 β , KC, and IL-6 in several isolated cell types mainly following LPS stimulation but also, when stimulated with IL-1 (3, 10, 24–27). However, our data here indicate that the contribution of Cot/tpl2 to the expression of a specific cytokine or chemokine *in vivo* is not as straightforward as detected in single isolated cell types. It is important to note that Cot/tpl2^{-/-} BMDM stimulated with zymosan show similar KC and MCP-1 secretion levels as reported previously for LPS-stimulated BMDM (data not shown). Indeed, and as expected in a dynamic process, our data indicate that the role of Cot/tpl2 on the production of certain inflammatory mediators varies during the inflammatory response. This hypothesis is reinforced by the fact that in the modulation of the hypernociceptive response the main striking difference is observed at 24 h, but differences in paw swelling by Cot/tpl2 deficiency are only observed at 3 h following the zymosan-induced inflammation response. Nevertheless, here we demonstrate that the expression levels of GM-CSF and G-CSF, with an active role in recruiting and maintain-

ing active macrophages and neutrophils at the inflammatory focus (54–56), are modulated by Cot/tpl2.

Cot/tpl2 has been proposed to be essential for the TNF α secretion in response to LPS stimulation. The prior intravenously administration of a Cot/tpl2 inhibitor in rats reduced TNF α plasma levels by 85% at 90 min following LPS administration (35). Besides, Cot/tpl2^{-/-} mice hardly produce any TNF α within the first 30 and 60 min after intraperitoneal injection of LPS/D-galactosamine (7). Furthermore, Cot/tpl2^{-/-} mice show a 50% decrease in TNF α levels in the peritoneum after 2 or 3 h of zymosan intraperitoneal injection (data not shown) (11). In contrast, in zymosan-induced intraplantar inflammation, Cot/tpl2 hardly regulates TNF α production within the first 5 h following zymosan injection, but a significant TNF α decrease by Cot/tpl2 deficiency is observed 24 h after the induction of inflammation.

Cot/tpl2 controls the production of PGE₂ in LPS-stimulated Cot/tpl2-deficient BMDM (62) as well as in IL-1 stimulated rheumatoid arthritis fibroblast-like synoviocytes (27). The expression of COX2 is impaired in zymosan-stimulated Cot/tpl2-deficient BMDM within the first 8 h of stimulation, as is PGE₂ production, although these data do not correlate with that observed *in vivo*. In this context, it is again clear that the tissue microenvironment is more complex than isolated cell systems. LTB₄ plays an important role in inflammatory hypernociception. It has been shown to mediate the secretion of PGE₂ in zymosan-induced inflammation *in vivo* (61), and zymosan induces LTB₄ in mast cells (65). Thus, considering the correlation between the levels of PGE₂ and LTB₄ during the course of hindpaw inflammation, it remains possible that PGE₂ levels that are increased in 5-h zymosan-injected Cot/tpl2^{-/-} hindpaws but decreased 24 h after zymosan injection are LTB₄-mediated.

Inflammatory hypernociception is directly dependent on the production of nociceptive mediators generated at the inflamed site (53, 66, 67). PGE₂, TNF α , NGF, IL-1 β , and IL-6 provoke the activation of nociceptive terminals that innervate the inflamed tissues (52, 53, 58). Our data show that Cot/tpl2 controls the production of NGF during the course of the zymosan-induced inflammation. Decreased levels of IL-1 β and IL-6 within the first 5 h after the intraplantar injection of zymosan in Cot/tpl2^{-/-} mice were also observed. At this time point, however, the Cot/tpl2^{-/-} mice reflected a reduction of only approximately 15% in the hypernociceptive behavior compared with WT littermates. In this context, it should be noted that at this time increased levels of PGE₂ in Cot/tpl2^{-/-} zymosan-injected hindpaws were detected. Nevertheless, 24 h following intraplantar injection of zymosan, Cot/tpl2^{-/-} mice showed a 50% reduction in the hypernociceptive behavior, together with reduced levels of NGF, TNF α , and PGE₂.

In conclusion, our data show that Cot/tpl2 regulates NGF and LTB₄ production, the levels of GM-CSF and G-CSF, and MPO activity along inflammatory response affecting the zymosan-induced acute inflammatory process and the resulting hypernociception.

Acknowledgments—We thank R. Encinar, C. Sánchez-Palomo, and M^aC. Moreno for the technical work, Carlos Avendaño for conceptual advice, and Eduardo Malmierca for the critical reading of the manuscript.

REFERENCES

- Takeuchi, O., and Akira, S. (2010) *Cell* **140**, 805–820
- Akira, S., and Takeda, K. (2004) *Nat. Rev. Immunol.* **4**, 499–511
- Banerjee, A., Gugasyan, R., McMahon, M., and Gerondakis, S. (2006) *Proc. Natl. Acad. Sci. U.S.A.* **103**, 3274–3279
- Banerjee, A., and Gerondakis, S. (2007) *Immunol. Cell Biol.* **85**, 420–424
- Loniewski, K. J., Patial, S., and Parameswaran, N. (2007) *Mol. Immunol.* **44**, 3715–3723
- Waterfield, M. R., Zhang, M., Norman, L. P., and Sun, S. C. (2003) *Mol. Cell* **11**, 685–694
- Dumitru, C. D., Ceci, J. D., Tsatsanis, C., Kontoyiannis, D., Stamatakis, K., Lin, J. H., Patriotis, C., Jenkins, N. A., Copeland, N. G., Kollias, G., and Tschlis, P. N. (2000) *Cell* **103**, 1071–1083
- Caivano, M., Rodriguez, C., Cohen, P., and Alemany, S. (2003) *J. Biol. Chem.* **278**, 52124–52130
- Eliopoulos, A. G., Dumitru, C. D., Wang, C. C., Cho, J., and Tschlis, P. N. (2002) *EMBO J.* **21**, 4831–4840
- Rodríguez, C., Pozo, M., Nieto, E., Fernández, M., and Alemany, S. (2006) *Cell. Signal.* **18**, 1376–1385
- Mielke, L. A., Elkins, K. L., Wei, L., Starr, R., Tschlis, P. N., O'Shea, J. J., and Watford, W. T. (2009) *J. Immunol.* **183**, 7984–7993
- Salmerón, A., Janzen, J., Soneji, Y., Bump, N., Kamens, J., Allen, H., and Ley, S. C. (2001) *J. Biol. Chem.* **276**, 22215–22222
- Heissmeyer, V., Krappmann, D., Wulczyn, F. G., and Scheidereit, C. (1999) *EMBO J.* **18**, 4766–4778
- Orian, A., Gonen, H., Bercovich, B., Fajerman, I., Eytan, E., Israël, A., Mercurio, F., Iwai, K., Schwartz, A. L., and Ciechanover, A. (2000) *EMBO J.* **19**, 2580–2591
- Vallabhapurapu, S., and Karin, M. (2009) *Annu. Rev. Immunol.* **27**, 693–733
- Stafford, M. J., Morrice, N. A., Pegg, M. W., and Cohen, P. (2006) *FEBS Lett.* **580**, 4010–4014
- Cho, J., and Tschlis, P. N. (2005) *Proc. Natl. Acad. Sci. U.S.A.* **102**, 2350–2355
- Robinson, M. J., Beinke, S., Kouroumalis, A., Tschlis, P. N., and Ley, S. C. (2007) *Mol. Cell Biol.* **27**, 7355–7364
- Handoyo, H., Stafford, M. J., McManus, E., Baltzis, D., Pegg, M., and Cohen, P. (2009) *Biochem. J.* **424**, 109–118
- Waterfield, M., Jin, W., Reiley, W., Zhang, M., and Sun, S. C. (2004) *Mol. Cell Biol.* **24**, 6040–6048
- Beinke, S., Deka, J., Lang, V., Belich, M. P., Walker, P. A., Howell, S., Smerdon, S. J., Gamblin, S. J., and Ley, S. C. (2003) *Mol. Cell Biol.* **23**, 4739–4752
- Beinke, S., and Ley, S. C. (2004) *Biochem. J.* **382**, 393–409
- Gándara, M. L., López, P., Hernando, R., Castaño, J. G., and Alemany, S. (2003) *Mol. Cell Biol.* **23**, 7377–7390
- Rousseau, S., Papoutsopoulou, M., Symons, A., Cook, D., Lucocq, J. M., Prescott, A. R., O'Garra, A., Ley, S. C., and Cohen, P. (2008) *J. Cell Sci.* **121**, 149–154
- Yang, H. T., Cohen, P., and Rousseau, S. (2008) *Cell. Signal.* **20**, 375–380
- Van Acker, G. J., Perides, G., Weiss, E. R., Das, S., Tschlis, P. N., and Steer, M. L. (2007) *J. Biol. Chem.* **282**, 22140–22149
- Hall, J. P., Kurdi, Y., Hsu, S., Cuzzo, J., Liu, J., Telliez, J. B., Seidl, K. J., Winkler, A., Hu, Y., Green, N., Askew, G. R., Tam, S., Clark, J. D., and Lin, L. L. (2007) *J. Biol. Chem.* **282**, 33295–33304
- Kontoyiannis, D., Boulougouris, G., Manoloukos, M., Armaka, M., Apostolaki, M., Pizarro, T., Kotlyarov, A., Forster, I., Flavell, R., Gaestel, M., Tschlis, P., Cominelli, F., and Kollias, G. (2002) *J. Exp. Med.* **196**, 1563–1574
- Cohen, P. (2009) *Curr. Opin. Cell Biol.* **21**, 317–324
- Gaestel, M., Kotlyarov, A., and Kracht, M. (2009) *Nat. Rev. Drug Discov.* **8**, 480–499
- Kaila, N., Green, N., Li, H. Q., Hu, Y., Janz, K., Gavrin, L. K., Thomason, J., Tam, S., Powell, D., Cuzzo, J., Hall, J. P., Telliez, J. B., Hsu, S., Nickerson-Nutter, C., Wang, Q., and Lin, L. L. (2007) *Bioorg. Med. Chem.* **15**, 6425–6442
- Cusack, K., Allen, H., Bischoff, A., Clabbers, A., Dixon, R., Fix-Stenzel, S., Friedman, M., Gaumont, Y., George, D., Gordon, T., Grongsaard, P., Jansen, B., Jia, Y., Moskey, M., Quinn, C., Salmeron, A., Thomas, C., Wallace, G., Wishart, N., and Yu, Z. (2009) *Bioorg. Med. Chem. Lett.* **19**, 1722–1725
- Li, Y. L., Torchet, C., Vergne, J., and Maurel, M. C. (2007) *Biochimie* **89**, 1257–1263
- Li, Y. L., Vergne, J., Torchet, C., and Maurel, M. C. (2009) *FEBS J.* **276**, 303–314
- Green, N., Hu, Y., Janz, K., Li, H. Q., Kaila, N., Guler, S., Thomason, J., Joseph-McCarthy, D., Tam, S. Y., Hotchandani, R., Wu, J., Huang, A., Wang, Q., Leung, L., Pelker, J., Marusic, S., Hsu, S., Telliez, J. B., Hall, J. P., Cuzzo, J. W., and Lin, L. L. (2007) *J. Med. Chem.* **50**, 4728–4745
- George, D., Friedman, M., Allen, H., Argiriadi, M., Barberis, C., Bischoff, A., Clabbers, A., Cusack, K., Dixon, R., Fix-Stenzel, S., Gordon, T., Janssen, B., Jia, Y., Moskey, M., Quinn, C., Salmeron, J. A., Wishart, N., Woller, K., and Yu, Z. (2008) *Bioorg. Med. Chem. Lett.* **18**, 4952–4955
- Rodríguez, C., López, P., Pozo, M., Duce, A. M., López-Pelaéz, M., Fernández, M., and Alemany, S. (2008) *Cell. Signal.* **20**, 1625–1631
- Giannini, E., Lattanzi, R., Nicotra, A., Campese, A. F., Grazioli, P., Screpanti, I., Balboni, G., Salvadori, S., Sacerdote, P., and Negri, L. (2009) *Proc. Natl. Acad. Sci. U.S.A.* **106**, 14646–14651
- Rittner, H. L., Brack, A., Machelsha, H., Mousa, S. A., Bauer, M., Schäfer, M., and Stein, C. (2001) *Anesthesiology* **95**, 500–508
- Perruche, S., Kleinclaus, F., Lienard, A., Robinet, E., Tiberghien, P., and Saas, P. (2004) *J. Immunol. Methods* **294**, 53–66
- Gross, S., Gammon, S. T., Moss, B. L., Rauch, D., Harding, J., Heinecke, J. W., Ratner, L., and Piwnicka-Worms, D. (2009) *Nat. Med.* **15**, 455–461
- Bhatia, M., Sidhapuriwala, J., Moochhala, S. M., and Moore, P. K. (2005) *Br. J. Pharmacol.* **145**, 141–144
- Traves, P. G., Hortelano, S., Zeini, M., Chao, T. H., Lam, T., Neuteboom, S. T., Theodorakis, E. A., Palladino, M. A., Castrillo, A., and Bosca, L. (2007) *Mol. Pharmacol.* **71**, 1545–1553
- Kingery, W. S., Guo, T., Agashe, G. S., Davies, M. F., Clark, J. D., and Maze, M. (2001) *Brain Res.* **913**, 140–148
- Gantner, B. N., Simmons, R. M., Canavera, S. J., Akira, S., and Underhill, D. M. (2003) *J. Exp. Med.* **197**, 1107–1117
- Bradley, P. P., Priebat, D. A., Christensen, R. D., and Rothstein, G. (1982) *J. Invest. Dermatol.* **78**, 206–209
- Haqqani, A. S., Sandhu, J. K., and Birnboim, H. C. (1999) *Anal. Biochem.* **273**, 126–132
- El Kebir, D., József, L., Pan, W., Wang, L., Petasis, N. A., Serhan, C. N., and Filep, J. G. (2009) *Am. J. Respir. Crit. Care Med.* **180**, 311–319
- Haegens, A., Heeringa, P., van Suylen, R. J., Steele, C., Aratani, Y., O'Donoghue, R. J., Mutsaers, S. E., Mossman, B. T., Wouters, E. F., and Vernooy, J. H. (2009) *J. Immunol.* **182**, 7990–7996
- El Kebir, D., József, L., Pan, W., and Filep, J. G. (2008) *Circ. Res.* **103**, 352–359
- Lau, D., Mollnau, H., Eiserich, J. P., Freeman, B. A., Daiber, A., Gehling, U. M., Brümmer, J., Rudolph, V., Münzel, T., Heitzer, T., Meinertz, T., and Baldus, S. (2005) *Proc. Natl. Acad. Sci. U.S.A.* **102**, 431–436
- Marchand, F., Perretti, M., and McMahon, S. B. (2005) *Nat. Rev. Neurosci.* **6**, 521–532
- Verri, W. A., Jr., Cunha, T. M., Parada, C. A., Poole, S., Cunha, F. Q., and Ferreira, S. H. (2006) *Pharmacol. Ther.* **112**, 116–138
- Coxon, A., Tang, T., and Mayadas, T. N. (1999) *J. Exp. Med.* **190**, 923–934
- Frossard, J. L., Saluja, A. K., Mach, N., Lee, H. S., Bhagat, L., Hadenque, A., Rubbia-Brandt, L., Dranoff, G., and Steer, M. L. (2002) *Am. J. Physiol. Lung Cell Mol. Physiol.* **283**, L541–L548
- Cowburn, A. S., Cadwallader, K. A., Reed, B. J., Farahi, N., and Chilvers, E. R. (2002) *Blood* **100**, 2607–2616
- Cunha, T. M., Verri, W. A., Jr., Silva, J. S., Poole, S., Cunha, F. Q., and Ferreira, S. H. (2005) *Proc. Natl. Acad. Sci. U.S.A.* **102**, 1755–1760
- McMahon, S. B. (1996) *Philos. Trans. R. Soc. Lond. B Biol. Sci.* **351**, 431–440
- Safieh-Garabedian, B., Poole, S., Allchorne, A., Winter, J., and Woolf, C. J. (1995) *Br. J. Pharmacol.* **115**, 1265–1275
- Woolf, C. J., Allchorne, A., Safieh-Garabedian, B., and Poole, S. (1997) *Br. J. Pharmacol.* **121**, 417–424

61. Guerrero, A. T., Verri, W. A., Jr., Cunha, T. M., Silva, T. A., Schivo, I. R., Dal-Secco, D., Canetti, C., Rocha, F. A., Parada, C. A., Cunha, F. Q., and Ferreira, S. H. (2008) *J. Leukocyte Biol.* **83**, 122–130
62. Eliopoulos, A. G., Davies, C., Blake, S. S., Murray, P., Najafipour, S., Tschlis, P. N., and Young, L. S. (2002) *J. Virol.* **76**, 4567–4579
63. Souza, G. E., Cunha, F. Q., Mello, R., and Ferreira, S. H. (1988) *Agents Actions* **24**, 377–380
64. Ribeiro, R. A., Souza-Filho, M. V., Souza, M. H., Oliveira, S. H., Costa, C. H., Cunha, F. Q., and Ferreira, H. S. (1997) *Int. Arch. Allergy Immunol.* **112**, 27–35
65. Olynych, T. J., Jakeman, D. L., and Marshall, J. S. (2006) *J. Allergy Clin. Immunol.* **118**, 837–843
66. Medzhitov, R. (2008) *Nature* **454**, 428–435
67. Verri, W. A., Jr., Cunha, T. M., Magro, D. A., Guerrero, A. T., Vieira, S. M., Carregaro, V., Souza, G. R., Henriques, M. G., Ferreira, S. H., and Cunha, F. Q. (2009) *Naunyn Schmiedebergs Arch. Pharmacol* **379**, 271–279